IEEE Access
Multidisciplinary | Rapid Review | Open Access Journal

Received January 22, 2020, accepted February 5, 2020, date of publication February 10, 2020, date of current version February 20, 2020.

Digital Object Identifier 10.1109/ACCESS.2020.2972998

Analysis of Elliptical Waveguides With Anisotropic Dielectric Layers

VEENU KAMRA, (Member, IEEE), AND ACHIM DREHER, (Senior Member, IEEE)
German Aerospace Center (DLR), Institute of Communications and Navigation, 82234 Wessling, Germany

Corresponding author: Veenu Kamra (veenu.kamra@dlr.de)

This work was supported by DLR/DAAD Research Fellowship.

ABSTRACT Our main objective is to extend the discrete mode matching (DMM) method to analyze multilayered elliptical fibers or transmission lines with elliptical dielectric layers. We generate the formulation for the full-wave equivalent circuit (FWEC) and derive the hybrid matrix elements for the dielectric layers in an elliptical coordinate system and then obtain the system equation of the structure. To demonstrate the technique, we analyze elliptical waveguides and compare the results with the data obtained by other authors and by commercial software.

INDEX TERMS Multilayered microwave structures, anisotropic media, conformal, numerical analysis.

I. INTRODUCTION

During the past decades, a considerable amount of attention has been paid to the analysis of optical fibers or dielectric waveguides for fast data transmission. The fibers exhibit ellipticity due to fabrication imperfections or purposely, due to manufacturing convenience. Also, the elliptical fibers have the interesting feature that their higher order modes are azimuthally stable, in contrast to circular fibers.

Several authors have analyzed elliptical waveguides in the literature, for example propagating modes are determined using ellipse transformation perturbation method (ETPM) in [1]. The cutoff wavelength is solved using the method of fundamental solutions (MFS) along with the singular value decomposition (SVD) technique in [2] and higher order mode cutoff is investigated in [3]. Reference [4] explained the analysis of elliptical fibers using the method of lines (MoL) in elliptical coordinates but the angular Mathieu functions are approximated with a Fourier expansion. Dyott collated lot of information on several approaches used to analyze elliptical fibers in his book [5]. Reference [6] also discussed in detail the fundamental theory of wave propagation in elliptical dielectric rods and several results in Chapter 6 of the book. Reference [7] developed the analytical expressions for reflection and transmission coefficients in elliptical cylinder using transfer matrix method. Reference [8] dealt with stripline structures mounted on elliptical cylinder using moment method and [9] used weakly guiding approach to solve propagation constants by solving Mathieu's equation.

The discrete mode matching method has been proven to be an efficient spectral or spatial domain numerical method for the full-wave analysis of multilayered microwave structures such as waveguides, striplines and microstrip antennas [10]–[13]. References [12] and [13] take into account anisotropic layered media in the structures. The method has the advantage that we need to discretize the transmission line structures only in one direction while we use the analytical solution in the remaining directions. Thus, we save a lot of computational time and effort compared to other numerical schemes. The increase in the discretization lines is equivalent to the increase in the number of modes used for the field expansion due to the Nyquist-Shannon sampling theorem. References [10], [11], [13] also discuss about the convergence of the DMM computations with respect to the discretization lines on the structure. DMM provides smooth convergence of the results. In [13], we have dealt with elliptical structures using a cylindrical coordinate system. The goal of this paper is to extend the DMM method to directly deal with an elliptical coordinate system. We consider the problem of electromagnetic wave propagation along a dielectric cylinder of elliptical cross-section. We use elliptic cylinder functions, known as Mathieu functions to find the solution of the Helmholtz equation. The whole analysis is done in spatial domain.

This paper first describes the solution of the Helmholtz equation in elliptical coordinates. Then, it explains the derivation of the hybrid-matrix elements for elliptical

The associate editor coordinating the review of this manuscript and approving it for publication was Giovanni Angiulli.

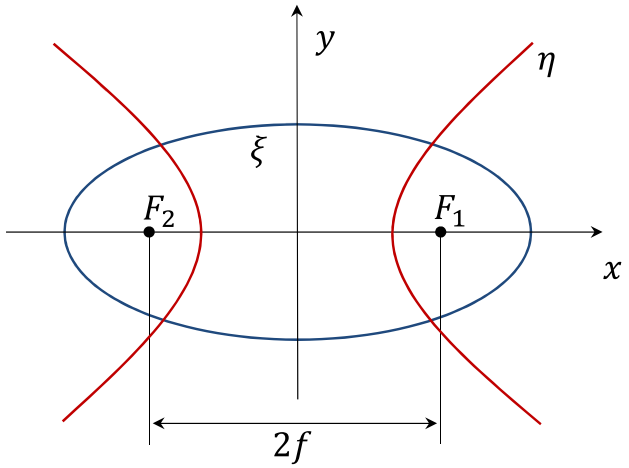

FIGURE 1. Elliptical cylindrical coordinates with semifocal length f.

dielectric layers. We demonstrate the application by computing propagation constants for elliptical dielectric waveguides with isotropic and uniaxial anisotropic layers. Finally, we validate the computed results with the open literature and/or results obtained from the commercial software ANSYS HFSS.

II. FORMULATION IN THE ELLIPTICAL COORDINATE SYSTEM

Let us consider the elliptical coordinate system (ξ, η, z) as shown in Fig. 1. In the figure, we describe the elliptical cylinder by the coordinate ξ and the hyperbolic cylinder by the coordinate η. We locate the two foci of the elliptical cylinder at $-f$ and $+f$ on the x-axis. We can write the relation between the Cartesian and the elliptical coordinate system as

$$x = f\cosh\xi\cos\eta = A\cos\eta, \tag{1}$$
$$y = f\sinh\xi\sin\eta = B\sin\eta, \tag{2}$$
$$z = z, \tag{3}$$

where A and B represent the major and minor semi-axes of the elliptical cylinder. The range of the coordinates is specified as

$$\xi \geq 0, \qquad 0 \leq \eta \leq 2\pi, \qquad -\infty < z < \infty. \tag{4}$$

A. SOLUTION OF MAXWELL'S EQUATIONS

We write Maxwell's equations in elliptical coordinates and for a source-free and homogeneous medium in their differential form as

$$\nabla \times \vec{E}(\xi,\eta,z) = -j\omega\bar{\bar{\mu}}\cdot\vec{H}(\xi,\eta,z), \tag{5a}$$
$$\nabla \times \vec{H}(\xi,\eta,z) = j\omega\bar{\bar{\varepsilon}}\cdot\vec{E}(\xi,\eta,z). \tag{5b}$$

where $\vec{E}$ and $\vec{H}$ are electric and magnetic field vectors, ω is the angular frequency. In elliptical coordinates, we write

$$\vec{E}(\xi,\eta,z) = E_\xi(\xi,\eta,z)\hat{\xi} + E_\eta(\xi,\eta,z)\hat{\eta} + E_z(\xi,\eta,z)\hat{z}, \tag{6}$$

with $\hat{\xi}$, $\hat{\eta}$ and $\hat{z}$ denoting the unit vectors along ξ, η and z coordinates, respectively. We suppress the time dependence $\exp(j\omega t)$ throughout this work. We take the permittivity ($\bar{\bar{\varepsilon}} = \varepsilon_0\bar{\bar{\varepsilon}}_r$) and permeability ($\bar{\bar{\mu}} = \mu_0\bar{\bar{\mu}}_r$) tensors with optical axis in z-direction with

$$\bar{\bar{\varepsilon}}_r = \begin{pmatrix} \varepsilon_t & 0 & 0 \\ 0 & \varepsilon_t & 0 \\ 0 & 0 & \varepsilon_z \end{pmatrix}, \quad \bar{\bar{\mu}}_r = \begin{pmatrix} \mu_t & 0 & 0 \\ 0 & \mu_t & 0 \\ 0 & 0 & \mu_z \end{pmatrix}. \tag{7}$$

As the optical axis is in z-direction, we assume E_z and H_z as the two independent field components. After expanding (5b) and doing some analytical work, we can calculate the other field components using the relations

$$\left(\frac{\partial^2}{\partial z^2} + \omega^2\varepsilon_0\mu_0\varepsilon_t\mu_t\right)E_\xi = \frac{1}{h}\frac{\partial}{\partial z}\frac{\partial}{\partial\xi}E_z - \frac{j\omega\mu_0\mu_t}{h}\frac{\partial}{\partial\eta}H_z \tag{8a}$$

$$\left(\frac{\partial^2}{\partial z^2} + \omega^2\varepsilon_0\mu_0\varepsilon_t\mu_t\right)H_\xi = \frac{j\omega\varepsilon_0\varepsilon_t}{h}\frac{\partial}{\partial\eta}E_z + \frac{1}{h}\frac{\partial}{\partial z}\frac{\partial}{\partial\xi}H_z \tag{8b}$$

$$\left(\frac{\partial^2}{\partial z^2} + \omega^2\varepsilon_0\mu_0\varepsilon_t\mu_t\right)E_\eta = \frac{1}{h}\frac{\partial}{\partial z}\frac{\partial}{\partial\eta}E_z + \frac{j\omega\mu_0\mu_t}{h}\frac{\partial}{\partial\xi}H_z \tag{8c}$$

$$\left(\frac{\partial^2}{\partial z^2} + \omega^2\varepsilon_0\mu_0\varepsilon_t\mu_t\right)H_\eta = \frac{-j\omega\varepsilon_0\varepsilon_t}{h}\frac{\partial}{\partial\xi}E_z + \frac{1}{h}\frac{\partial}{\partial z}\frac{\partial}{\partial\eta}H_z. \tag{8d}$$

Here the scale factor $h = f\sqrt{\cosh^2\xi - \cos^2\eta}$ and $f = \sqrt{(A^2 - B^2)}$ represents the semifocal length of the ellipse.

We write the source free differential equation for the electric field E_z in elliptical coordinates as

$$\left(\frac{\partial^2}{\partial\xi^2} + \frac{\partial^2}{\partial\eta^2} + h^2\frac{\varepsilon_z}{\varepsilon_t}\frac{\partial^2}{\partial z^2} + h^2\omega^2\varepsilon_0\mu_0\mu_t\varepsilon_z\right)E_z = 0, \tag{9}$$

and for the magnetic field H_z as

$$\left(\frac{\partial^2}{\partial\xi^2} + \frac{\partial^2}{\partial\eta^2} + h^2\frac{\mu_z}{\mu_t}\frac{\partial^2}{\partial z^2} + h^2\omega^2\varepsilon_0\mu_0\varepsilon_t\mu_z\right)H_z = 0. \tag{10}$$

On assuming that the propagation is in z-direction then the equations lead to

$$\left(\frac{\partial^2}{\partial\xi^2} + \frac{\partial^2}{\partial\eta^2} + h^2\varepsilon_{d(e,h)}\right)\psi = 0, \tag{11}$$

where ψ represents each of the independent electromagnetic field components, i.e., $E_z(\xi,\eta)$ and $H_z(\xi,\eta)$ and $\varepsilon_{de} = \omega^2\varepsilon_0\mu_0\mu_t\varepsilon_z - k_z^2\varepsilon_z/\varepsilon_t$ and $\varepsilon_{dh} = \omega^2\varepsilon_0\mu_0\varepsilon_t\mu_z - k_z^2\mu_z/\mu_t$ for E_z and H_z, respectively. Here, k_z is the propagation constant in z-direction. Similar to the procedure explained in [6], we apply next the rule of separation of variables on the field components and set

$$\psi = R(\xi)S(\eta). \tag{12}$$

Then we obtain two ordinary differential equations

$$\frac{\partial^2 S(\eta)}{\partial\eta^2} + (a - 2q\cos 2\eta)S(\eta) = 0, \tag{13}$$
$$\frac{\partial^2 R(\xi)}{\partial\xi^2} - (a - 2q\cosh 2\xi)R(\xi) = 0. \tag{14}$$

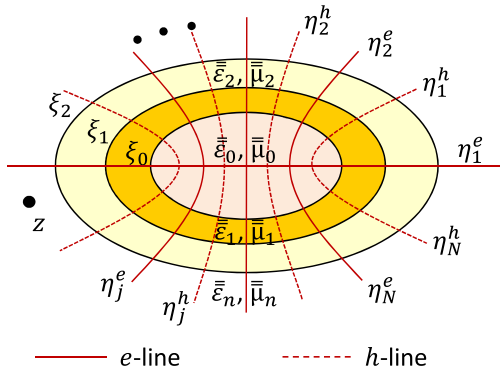

(a) Layers with equal ellipticities.

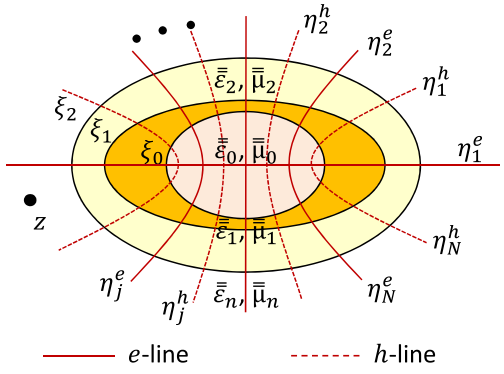

(b) Layers with different ellipticities.

FIGURE 2. The elliptical transmission lines with discretization scheme.

Here, a represents the separation constant and q equals $\varepsilon_{de}f^2/4$ (or q_e) and $\varepsilon_{dh}f^2/4$ (or q_h) for E_z and H_z, respectively. These equations are known as Mathieu differential equation and modified Mathieu differential equation, respectively.

Fig. 2 shows elliptical transmission lines with layered dielectric media with same and different ellipticities. Ellipticity of the interface can be defined by $e = f/A$. We need the field components for inner layer 0 extending from $\xi = 0$ to ξ_0, for arbitrary layer k extending from $\xi = \xi_{k-1}$ to ξ_k and for outer layer n extending from $\xi = \xi_{n-1}$ to ∞ as shown in the figure. We express the solution of the differential equation (9) as linear combination of products of angular and radial Mathieu functions:

$$\begin{aligned} E_{z_0} &= \sum_{i=0}^{\infty} A_{0_i}\mathrm{Je}_i(q_{e_{0,0}},\xi)\mathrm{Ce}_i(q_{e_{0,0}},\eta) \\ &\quad + \sum_{i=1}^{\infty} B_{0_i}\mathrm{Jo}_i(q_{e_{0,0}},\xi)\mathrm{So}_i(q_{e_{0,0}},\eta) \\ &\quad (0 \le \xi \le \xi_0), \qquad (15) \\ E_{z_k} &= \sum_{i=0}^{\infty}[A_{k1_i}\mathrm{Je}_i(q_{e_{k,int}},\xi) + A_{k2_i}\mathrm{Ne}_i(q_{e_{k,int}},\xi)] \\ &\quad \mathrm{Ce}_i(q_{e_{k,int}},\eta) + \sum_{i=1}^{\infty}[B_{k1_i}\mathrm{Jo}_i(q_{e_{k,int}},\xi) \\ &\quad + B_{k2_i}\mathrm{No}_i(q_{e_{k,int}},\xi)]\mathrm{So}_i(q_{e_{k,int}},\eta) \\ &\quad (\xi_{k-1} \le \xi \le \xi_k), \qquad (16) \end{aligned}$$

$$\begin{aligned} E_{z_n} &= \sum_{i=0}^{\infty} A_{n_i}\mathrm{He}_i^{(2)}(q_{e_{n,n-1}},\xi)\mathrm{Ce}_i(q_{e_{n,n-1}},\eta) \\ &\quad + \sum_{i=1}^{\infty} B_{n_i}\mathrm{Ho}_i^{(2)}(q_{e_{n,n-1}},\xi)\mathrm{So}_i(q_{e_{n,n-1}},\eta) \\ &\quad (\xi_{n-1} \le \xi < \infty). \qquad (17) \end{aligned}$$

Similarly, we write the solution of the differential equation (10) as

$$\begin{aligned} H_{z_0} &= \sum_{i=0}^{\infty} C_{0_i}\mathrm{Je}_i(q_{h_{0,0}},\xi)\mathrm{Ce}_i(q_{h_{0,0}},\eta) \\ &\quad + \sum_{i=1}^{\infty} D_{0_i}\mathrm{Jo}_i(q_{h_{0,0}},\xi)\mathrm{So}_i(q_{h_{0,0}},\eta) \\ &\quad (0 \le \xi \le \xi_0), \qquad (18) \\ H_{z_k} &= \sum_{i=0}^{\infty}[C_{k1_i}\mathrm{Je}_i(q_{h_{k,int}},\xi) + C_{k2_i}\mathrm{Ne}_i(q_{h_{k,int}},\xi)] \\ &\quad \mathrm{Ce}_i(q_{h_{k,int}},\eta) + \sum_{i=1}^{\infty}[D_{k1_i}\mathrm{Jo}_i(q_{h_{k,int}},\xi) \\ &\quad + D_{k2_i}\mathrm{No}_i(q_{h_{k,int}},\xi)]\mathrm{So}_i(q_{h_{k,int}},\eta) \\ &\quad (\xi_{k-1} \le \xi \le \xi_k), \qquad (19) \\ H_{z_n} &= \sum_{i=0}^{\infty} C_{n_i}\mathrm{He}_i^{(2)}(q_{h_{n,n-1}},\xi)\mathrm{Ce}_i(q_{h_{n,n-1}},\eta) \\ &\quad + \sum_{i=1}^{\infty} D_{n_i}\mathrm{Ho}_i^{(2)}(q_{h_{n,n-1}},\xi)\mathrm{So}_i(q_{h_{n,n-1}},\eta) \\ &\quad (\xi_{n-1} \le \xi < \infty). \qquad (20) \end{aligned}$$

The even and odd angular Mathieu functions, represented with Ce and So, respectively, are solutions of the Mathieu differential equation (13). The functions Je, Jo and Ne, No are radial Mathieu functions of the first and second kind which come from the solution of the modified Mathieu differential equation (14). They play a similar role as Bessel functions in the circular coordinate system. Eqs. (17) and (20) contain $\mathrm{He}^{(2)}$ and $\mathrm{Ho}^{(2)}$, which represent even and odd Mathieu-Hankel functions of the second kind, respectively, which are analogous to the Hankel functions. Mathieu-Hankel functions come from the solution of the modified Mathieu differential equation (14) in an unbounded domain. The angular Mathieu functions are expressed with Fourier series and the radial Mathieu functions as series of Bessel functions. Here the terms $q_{e_{k,int}}$ and $q_{h_{k,int}}$ are dependent on medium parameters with k denoting the dielectric layers and int denoting the interfaces between the layers. For example, layer 0 has only top interface 0 with $\xi = \xi_0$, layer k has both bottom and top interfaces represented by $k-1$ with $\xi = \xi_{k-1}$ and k with $\xi = \xi_k$, respectively, and layer n has bottom interface $n-1$ with $\xi = \xi_{n-1}$. Therefore, the Mathieu functions are not only functions of η or ξ coordinates, but also depend on the medium parameters, i.e., $\bar{\bar{\varepsilon}}$, $\bar{\bar{\mu}}$. The definitions of these Mathieu functions are given in [14]. The comparison between the notations are given in Table 1. The coefficients

TABLE 1. Comparative notations of the Mathieu functions.

This paper	Ce	So	Je	Jo	Ne	No	He	Ho
[14]	ce	se	Ce	Se	Fey	Gey	Me	Ne

are represented by A_{k1_i}, A_{k2_i}, A_{0_i}, A_{n_i}, B_{k1_i}, B_{k2_i}, B_{0_i}, B_{n_i}, C_{k1_i}, C_{k2_i}, C_{0_i}, C_{n_i}, D_{k1_i}, D_{k2_i}, D_{0_i} and D_{n_i} for mode i.

B. MODE CLASSIFICATION

We know that the coexistence of TE and TM modes happens when the fields are dependent on the angular coordinate. They give rise to the hybrid modes which are also the case in the cylindrical coordinate system. The modes are known as HE if the cross-sectional field pattern is similar to the TE mode or H mode, and EH if the cross-sectional field pattern is similar to the TM mode or E mode. However, there exists an asymmetry in the elliptical cylinder, which generates two types of field configurations. Thus, we have even or odd types of hybrid modes which are denoted with prescript e or o, i.e., e,oHE or e,oEH. The characteristic equations for odd and even hybrid modes for isotropic material are also derived in [15].

1) EVEN MODES

The expressions for the independent electric and magnetic field components for even modes eHE or eEH are

$$E_{z_0} = \sum_{i=1}^{\infty} B_{0_i}\mathrm{Jo}_i(q_{e_{0,0}},\xi)\mathrm{So}_i(q_{e_{0,0}},\eta) \quad (0 \le \xi \le \xi_0), \tag{21}$$

$$E_{z_k} = \sum_{i=1}^{\infty}[B_{k1_i}\mathrm{Jo}_i(q_{e_{k,int}},\xi) + B_{k2_i}\mathrm{No}_i(q_{e_{k,int}},\xi)] \mathrm{So}_i(q_{e_{k,int}},\eta) \quad (\xi_{k-1} \le \xi \le \xi_k), \tag{22}$$

$$E_{z_n} = \sum_{i=1}^{\infty} B_{n_i}\mathrm{Ho}_i^{(2)}(q_{e_{n,n-1}},\xi)\mathrm{So}_i(q_{e_{n,n-1}},\eta) \quad (\xi_{n-1} \le \xi < \infty), \tag{23}$$

$$H_{z_0} = \sum_{i=0}^{\infty} C_{0_i}\mathrm{Je}_i(q_{h_{0,0}},\xi)\mathrm{Ce}_i(q_{h_{0,0}},\eta) \quad (0 \le \xi \le \xi_0), \tag{24}$$

$$H_{z_k} = \sum_{i=0}^{\infty}[C_{k1_i}\mathrm{Je}_i(q_{h_{k,int}},\xi) + C_{k2_i}\mathrm{Ne}_i(q_{h_{k,int}},\xi)] \mathrm{Ce}_i(q_{h_{k,int}},\eta) \quad (\xi_{k-1} \le \xi \le \xi_k), \tag{25}$$

$$H_{z_n} = \sum_{i=0}^{\infty} C_{n_i}\mathrm{He}_i^{(2)}(q_{h_{n,n-1}},\xi)\mathrm{Ce}_i(q_{h_{n,n-1}},\eta) \quad (\xi_{n-1} \le \xi < \infty). \tag{26}$$

2) ODD MODES

Similarly, the expressions for the independent electric and magnetic field components for odd modes oHE or oEH are

$$E_{z_0} = \sum_{i=0}^{\infty} A_{0_i}\mathrm{Je}_i(q_{e_{0,0}},\xi)\mathrm{Ce}_i(q_{e_{0,0}},\eta) \quad (0 \le \xi \le \xi_0), \tag{27}$$

$$E_{z_k} = \sum_{i=0}^{\infty}[A_{k1_i}\mathrm{Je}_i(q_{e_{k,int}},\xi) + A_{k2_i}\mathrm{Ne}_i(q_{e_{k,int}},\xi)] \mathrm{Ce}_i(q_{e_{k,int}},\eta) \quad (\xi_{k-1} \le \xi \le \xi_k), \tag{28}$$

$$E_{z_n} = \sum_{i=0}^{\infty} A_{n_i}\mathrm{He}_i^{(2)}(q_{e_{n,n-1}},\xi)\mathrm{Ce}_i(q_{e_{n,n-1}},\eta) \quad (\xi_{n-1} \le \xi < \infty), \tag{29}$$

$$H_{z_0} = \sum_{i=1}^{\infty} D_{0_i}\mathrm{Jo}_i(q_{h_{0,0}},\xi)\mathrm{So}_i(q_{h_{0,0}},\eta) \quad (0 \le \xi \le \xi_0), \tag{30}$$

$$H_{z_k} = \sum_{i=1}^{\infty}[D_{k1_i}\mathrm{Jo}_i(q_{h_{k,int}},\xi) + D_{k2_i}\mathrm{No}_i(q_{h_{k,int}},\xi)] \mathrm{So}_i(q_{h_{k,int}},\eta) \quad (\xi_{k-1} \le \xi \le \xi_k), \tag{31}$$

$$H_{z_n} = \sum_{i=1}^{\infty} D_{n_i}\mathrm{Ho}_i^{(2)}(q_{h_{n,n-1}},\xi)\mathrm{So}_i(q_{h_{n,n-1}},\eta) \quad (\xi_{n-1} \le \xi < \infty). \tag{32}$$

C. THE DISCRETE MODE MATCHING METHOD

We assume that the structure is infinite in the propagation direction, i.e., in z-direction. From (21)-(26) and (27)-(32), it is clear that the wave solution for every elliptical cylinder ξ is dependent on each and every point on the η-axis. Therefore we do 1D discretization in the η-direction (see Fig. 2). For every value of q, there exists an infinite sequence of eigenvalues a and for each value of a exists a corresponding infinite sequence of eigenvectors (expansion coefficients). The important step in the algorithm is to compute the eigenvalues and the corresponding eigenvectors. Here, we consider a number of 25 expansion coefficients by default for all categories of Mathieu functions. In our code, we calculate exact expansion coefficients without any approximations.

We take E_z and H_z to be the two independent field components. We assume that E_z is sampled on e-lines and H_z on h-lines. We discretize the structure with N_η^e e-lines and N_η^h h-lines in the η-direction and include the same number of modes in the field expansion. Therefore, we write (21)-(26) in discretized form as

$$E_{z_0}(\xi,\eta_j^e) = \sum_{i=1}^{N_\eta^e} B_{0_i}\mathrm{Jo}_i(q_{e_{0,0}},\xi)\mathrm{So}_i(q_{e_{0,0}},\eta_j^e) \quad (0 \le \xi \le \xi_0), \tag{33}$$

$$E_{z_k}(\xi,\eta_j^e) = \sum_{i=1}^{N_\eta^e}[B_{k1_i}\mathrm{Jo}_i(q_{e_{k,int}},\xi) + B_{k2_i}\mathrm{No}_i(q_{e_{k,int}},\xi)] \mathrm{So}_i(q_{e_{k,int}},\eta_j^e) \quad (\xi_{k-1} \le \xi \le \xi_k), \tag{34}$$

$$E_{z_n}(\xi,\eta_j^e) = \sum_{i=1}^{N_\eta^e} B_{n_i}\mathrm{Ho}_i^{(2)}(q_{e_{n,n-1}},\xi)\mathrm{So}_i(q_{e_{n,n-1}},\eta_j^e) \quad (\xi_{n-1} \le \xi < \infty), \tag{35}$$

$$H_{z_0}(\xi,\eta_j^h) = \sum_{i=0}^{N_\eta^h} C_{0_i}\mathrm{Je}_i(q_{h_{0,0}},\xi)\mathrm{Ce}_i(q_{h_{0,0}},\eta_j^h) \quad (0 \le \xi \le \xi_0), \tag{36}$$

$$H_{z_k}(\xi,\eta_j^h)=\sum_{i=0}^{N_\eta^h}[C_{k1_i}\mathrm{Je}_i(q_{h_{k,int}},\xi)+C_{k2_i}\mathrm{Ne}_i(q_{h_{k,int}},\xi)]\,\mathrm{Ce}_i(q_{h_{k,int}},\eta_j^h)\quad(\xi_{k-1}\le\xi\le\xi_k),\tag{37}$$

$$H_{z_n}(\xi,\eta_j^h)=\sum_{i=0}^{N_\eta^h}C_{n_i}\mathrm{He}_i^{(2)}(q_{h_{n,n-1}},\xi)\mathrm{Ce}_i(q_{h_{n,n-1}},\eta_j^h)\quad(\xi_{n-1}\le\xi<\infty).\tag{38}$$

Similarly we can also write (27)-(32) in discretized form.

From (8), we can identify the location of the other field components. Therefore, we say that for 1D discretization E_z, E_ξ and H_η (or H_z, H_ξ and E_η) components are sampled at the same locations. Using (34), (37) and the field relations from Maxwell's equations, we write the discretized tangential field components for even modes in layer k in matrix form as

$$\begin{bmatrix}\boldsymbol{E}_{\eta_k}\\ \boldsymbol{H}_{\eta_k}\\ \boldsymbol{E}_{z_k}\\ \boldsymbol{H}_{z_k}\end{bmatrix}=\begin{bmatrix}\boldsymbol{Q}_{\eta_k}^{B_1} & \boldsymbol{Q}_{\eta_k}^{B_2} & \boldsymbol{Q}_{\eta_k}^{C_1} & \boldsymbol{Q}_{\eta_k}^{C_2}\\ \boldsymbol{G}_{\eta_k}^{B_1} & \boldsymbol{G}_{\eta_k}^{B_2} & \boldsymbol{G}_{\eta_k}^{C_1} & \boldsymbol{G}_{\eta_k}^{C_2}\\ \boldsymbol{Q}_{z_k}^{B_1} & \boldsymbol{Q}_{z_k}^{B_2} & \boldsymbol{0} & \boldsymbol{0}\\ \boldsymbol{0} & \boldsymbol{0} & \boldsymbol{G}_{z_k}^{C_1} & \boldsymbol{G}_{z_k}^{C_2}\end{bmatrix}\begin{bmatrix}\boldsymbol{B}_{k1}\\ \boldsymbol{B}_{k2}\\ \boldsymbol{C}_{k1}\\ \boldsymbol{C}_{k2}\end{bmatrix}.\tag{39}$$

Similarly, for odd modes

$$\begin{bmatrix}\boldsymbol{E}_{\eta_k}\\ \boldsymbol{H}_{\eta_k}\\ \boldsymbol{E}_{z_k}\\ \boldsymbol{H}_{z_k}\end{bmatrix}=\begin{bmatrix}\boldsymbol{Q}_{\eta_k}^{A_1} & \boldsymbol{Q}_{\eta_k}^{A_2} & \boldsymbol{Q}_{\eta_k}^{D_1} & \boldsymbol{Q}_{\eta_k}^{D_2}\\ \boldsymbol{G}_{\eta_k}^{A_1} & \boldsymbol{G}_{\eta_k}^{A_2} & \boldsymbol{G}_{\eta_k}^{D_1} & \boldsymbol{G}_{\eta_k}^{D_2}\\ \boldsymbol{Q}_{z_k}^{A_1} & \boldsymbol{Q}_{z_k}^{A_2} & \boldsymbol{0} & \boldsymbol{0}\\ \boldsymbol{0} & \boldsymbol{0} & \boldsymbol{G}_{z_k}^{D_1} & \boldsymbol{G}_{z_k}^{D_2}\end{bmatrix}\begin{bmatrix}\boldsymbol{A}_{k1}\\ \boldsymbol{A}_{k2}\\ \boldsymbol{D}_{k1}\\ \boldsymbol{D}_{k2}\end{bmatrix}.\tag{40}$$

Therefore, we write the relations for layer k in the form

$$\begin{bmatrix}\boldsymbol{E}_{k-1}\\ \boldsymbol{H}_{k-1}\end{bmatrix}=\boldsymbol{M}_{k-1}\boldsymbol{F},\quad\begin{bmatrix}\boldsymbol{E}_{k}\\ \boldsymbol{H}_{k}\end{bmatrix}=\boldsymbol{M}_{k}\boldsymbol{F},\tag{41}$$

where

$$\boldsymbol{M}_k=\begin{bmatrix}\boldsymbol{Q}_{\eta_k}^{B_1} & \boldsymbol{Q}_{\eta_k}^{B_2} & \boldsymbol{Q}_{\eta_k}^{C_1} & \boldsymbol{Q}_{\eta_k}^{C_2}\\ \boldsymbol{Q}_{z_k}^{B_1} & \boldsymbol{Q}_{z_k}^{B_2} & \boldsymbol{0} & \boldsymbol{0}\\ \boldsymbol{0} & \boldsymbol{0} & \boldsymbol{G}_{z_k}^{C_1} & \boldsymbol{G}_{z_k}^{C_2}\\ \boldsymbol{G}_{\eta_k}^{B_1} & \boldsymbol{G}_{\eta_k}^{B_2} & \boldsymbol{G}_{\eta_k}^{C_1} & \boldsymbol{G}_{\eta_k}^{C_2}\end{bmatrix}\tag{42}$$

for even modes and

$$\boldsymbol{M}_k=\begin{bmatrix}\boldsymbol{Q}_{\eta_k}^{A_1} & \boldsymbol{Q}_{\eta_k}^{A_2} & \boldsymbol{Q}_{\eta_k}^{D_1} & \boldsymbol{Q}_{\eta_k}^{D_2}\\ \boldsymbol{Q}_{z_k}^{A_1} & \boldsymbol{Q}_{z_k}^{A_2} & \boldsymbol{0} & \boldsymbol{0}\\ \boldsymbol{0} & \boldsymbol{0} & \boldsymbol{G}_{z_k}^{D_1} & \boldsymbol{G}_{z_k}^{D_2}\\ \boldsymbol{G}_{\eta_k}^{A_1} & \boldsymbol{G}_{\eta_k}^{A_2} & \boldsymbol{G}_{\eta_k}^{D_1} & \boldsymbol{G}_{\eta_k}^{D_2}\end{bmatrix}\tag{43}$$

for odd modes. We take the notations of the fields and coefficients in the matrix form as

$$\boldsymbol{E}_k=\begin{bmatrix}\boldsymbol{E}_{\eta_k}\\ \boldsymbol{E}_{z_k}\end{bmatrix},\ \boldsymbol{H}_k=\begin{bmatrix}\boldsymbol{H}_{z_k}\\ \boldsymbol{H}_{\eta_k}\end{bmatrix},\tag{44}$$

$$\boldsymbol{F}=\begin{bmatrix}\boldsymbol{B}_{k1}\\ \boldsymbol{B}_{k2}\\ \boldsymbol{C}_{k1}\\ \boldsymbol{C}_{k2}\end{bmatrix}\ \text{or}\ \begin{bmatrix}\boldsymbol{A}_{k1}\\ \boldsymbol{A}_{k2}\\ \boldsymbol{D}_{k1}\\ \boldsymbol{D}_{k2}\end{bmatrix}.\tag{45}$$

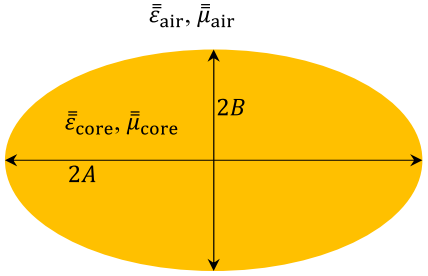

FIGURE 3. Schematic of elliptical waveguide cross-section.

After eliminating the unknown coefficient column matrix $\boldsymbol{F}$, it results in

$$\begin{bmatrix}\boldsymbol{E}_{k-1}\\ \boldsymbol{H}_{k-1}\end{bmatrix}=\boldsymbol{K}_k\begin{bmatrix}\boldsymbol{E}_{k}\\ \boldsymbol{H}_{k}\end{bmatrix}.\tag{46}$$

Therefore, we represent the hybrid matrix $\boldsymbol{K}_k$ for layer k as

$$\boldsymbol{K}_k=\boldsymbol{M}_{k-1}\boldsymbol{M}_k^{-1}.\tag{47}$$

Next on using (33), (36), (35) and (38), we write the discretized tangential field components present in the inner layer extending from $\xi=0$ to $\xi=\xi_0$ or outer unbounded layer for even modes as

$$\begin{bmatrix}\boldsymbol{E}_{\eta_\chi}\\ \boldsymbol{E}_{z_\chi}\end{bmatrix}=\begin{bmatrix}\boldsymbol{Q}_{\eta_\chi}^{B} & \boldsymbol{Q}_{\eta_\chi}^{C}\\ \boldsymbol{Q}_{z_\chi}^{B} & \boldsymbol{0}\end{bmatrix}\begin{bmatrix}\boldsymbol{B}_{\chi}\\ \boldsymbol{C}_{\chi}\end{bmatrix},\tag{48}$$

$$\begin{bmatrix}\boldsymbol{H}_{z_\chi}\\ \boldsymbol{H}_{\eta_\chi}\end{bmatrix}=\begin{bmatrix}\boldsymbol{0} & \boldsymbol{G}_{z_\chi}^{C}\\ \boldsymbol{G}_{\eta_\chi}^{B} & \boldsymbol{G}_{\eta_\chi}^{C}\end{bmatrix}\begin{bmatrix}\boldsymbol{B}_{\chi}\\ \boldsymbol{C}_{\chi}\end{bmatrix}.\tag{49}$$

For odd modes, we write

$$\begin{bmatrix}\boldsymbol{E}_{\eta_\chi}\\ \boldsymbol{E}_{z_\chi}\end{bmatrix}=\begin{bmatrix}\boldsymbol{Q}_{\eta_\chi}^{A} & \boldsymbol{Q}_{\eta_\chi}^{D}\\ \boldsymbol{Q}_{z_\chi}^{A} & \boldsymbol{0}\end{bmatrix}\begin{bmatrix}\boldsymbol{A}_{\chi}\\ \boldsymbol{D}_{\chi}\end{bmatrix},\tag{50}$$

$$\begin{bmatrix}\boldsymbol{H}_{z_\chi}\\ \boldsymbol{H}_{\eta_\chi}\end{bmatrix}=\begin{bmatrix}\boldsymbol{0} & \boldsymbol{G}_{z_\chi}^{D}\\ \boldsymbol{G}_{\eta_\chi}^{A} & \boldsymbol{G}_{\eta_\chi}^{D}\end{bmatrix}\begin{bmatrix}\boldsymbol{A}_{\chi}\\ \boldsymbol{D}_{\chi}\end{bmatrix},\tag{51}$$

where $\chi=0$ for inner layer and $\chi=n$ for the outer unbounded medium. We calculate the admittance by

$$\boldsymbol{Y}_\chi=\boldsymbol{M}_{H_\chi}\boldsymbol{M}_{E_\chi}^{-1},\tag{52}$$

where

$$\boldsymbol{M}_{E_\chi}=\begin{bmatrix}\boldsymbol{Q}_{\eta_\chi}^{B} & \boldsymbol{Q}_{\eta_\chi}^{C}\\ \boldsymbol{Q}_{z_\chi}^{B} & \boldsymbol{0}\end{bmatrix}\ \text{and}\ \boldsymbol{M}_{H_\chi}=\begin{bmatrix}\boldsymbol{0} & \boldsymbol{G}_{z_\chi}^{C}\\ \boldsymbol{G}_{\eta_\chi}^{B} & \boldsymbol{G}_{\eta_\chi}^{C}\end{bmatrix}\tag{53}$$

for even modes and

$$\boldsymbol{M}_{E_\chi}=\begin{bmatrix}\boldsymbol{Q}_{\eta_\chi}^{A} & \boldsymbol{Q}_{\eta_\chi}^{D}\\ \boldsymbol{Q}_{z_\chi}^{A} & \boldsymbol{0}\end{bmatrix}\ \text{and}\ \boldsymbol{M}_{H_\chi}=\begin{bmatrix}\boldsymbol{0} & \boldsymbol{G}_{z_\chi}^{D}\\ \boldsymbol{G}_{\eta_\chi}^{A} & \boldsymbol{G}_{\eta_\chi}^{D}\end{bmatrix}\tag{54}$$

for odd modes.

Let us consider a two-layer dielectric waveguide as shown in Fig. 3. We need to analyze only half of the structure due to symmetry. We get even modes by placing electric walls (E-wall) on the bounding domain while we get odd modes by placing magnetic walls (H-wall) on the boundary, as represented in Fig. 4. We can also analyze only a quarter

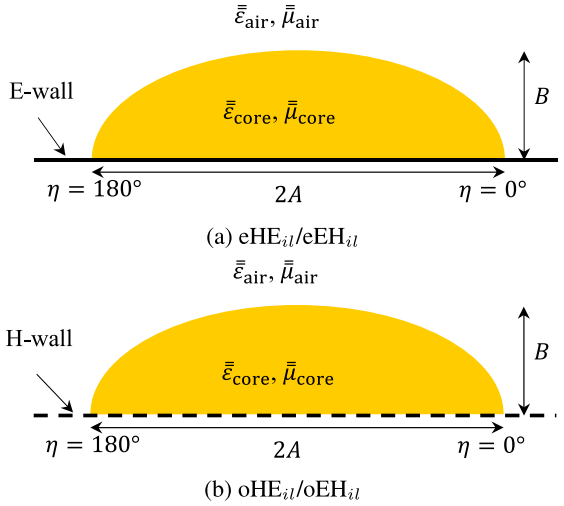

FIGURE 4. Half of the elliptical waveguide cross-section.

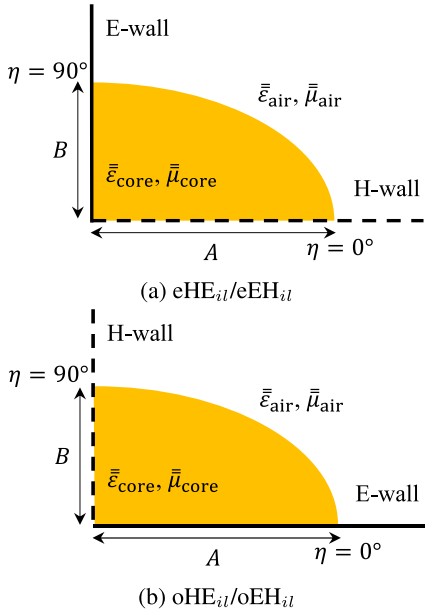

FIGURE 5. One quarter of the elliptical waveguide cross-section (*i* as odd index).

of the structure to get odd or even modes with odd subscript, e.g., eHE_{il} with i as odd index. Fig 5 gives the position of E- and H-walls to get suitable modes. Here the coordinate η discretization starts from the horizontal line, as given in Fig. 2. Table 2 defines the suitable values for mode i in the modal expansion for various boundary conditions.

After calculating the hybrid or admittance matrices for each dielectric layer, we calculate the system equation using a full-wave equivalent circuit [16] in the form

$$\boldsymbol{GJ} = \boldsymbol{E}. \tag{55}$$

Here the square matrix $\boldsymbol{G}$ represents the Green's function and the column matrices $\boldsymbol{J}$ and $\boldsymbol{E}$ represent surface current density and electric field in the interfaces, respectively. For waveguides $\boldsymbol{J} = 0$, therefore system equation reduces to

$$\boldsymbol{LE} = \boldsymbol{0}, \tag{56}$$

TABLE 2. Value of modes for different boundary combinations.

Boundary combination (left/right)	i (integers)
E/E	all(i)
M/M	all(i)
M/E	odd(i)

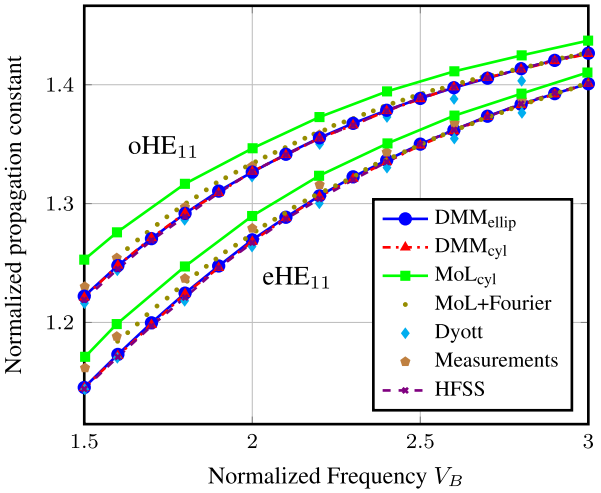

FIGURE 6. Dispersion curve of elliptical waveguide with isotropic material. (DMM_{cyl}: [13], MoL_{cyl}: [17], MoL+Fourier: [4], Dyott, Measurements: [5]).

where $\boldsymbol{L} = \boldsymbol{G}^{-1}$. Then, we find the propagation constant by solving the indirect eigenvalue problem (56). It can be done by varying the eigenvalue (propagation constant) until the determinant of the system matrix vanishes, i.e.,

$$\det \boldsymbol{L} = 0. \tag{57}$$

III. NUMERICAL RESULTS

A. ELLIPTICAL WAVEGUIDE

To validate the DMM formulations in elliptical coordinates, we have analyzed an elliptical dielectric waveguide. The waveguide comprises two layers, one is the elliptical core and the other is air surrounding the core as given in Fig. 3. The analysis is performed with an axial ratio $B/A = 0.5$, where B is the minor axis and A is the major axis. The material of the elliptical core is taken as $\varepsilon_{r,\text{core}} = (1.539)^2$ for the isotropic and $\bar{\bar{\varepsilon}}_{r,\text{core}} = ((1.539)^2, (1.539)^2, (1.25)^2)$ for the anisotropic case. The dispersion curves, as shown in Fig. 6 and 7, are plotted against the normalized frequency $V_B = Bk_0\sqrt{\varepsilon_{r,\text{core}} - \varepsilon_{r,\text{air}}}$. Here V_B is calculated using isotropic values for both the isotropic and the anisotropic case. The computed propagation constants are normalized with the free-space wave number k_0. Fig. 8 gives the numerical solution of the determinantal equation (57) at $V_B = 1.5$ for anisotropic case. We get two separate curves when only half of the waveguide is analyzed with even or odd case separately as specified in the theory section.

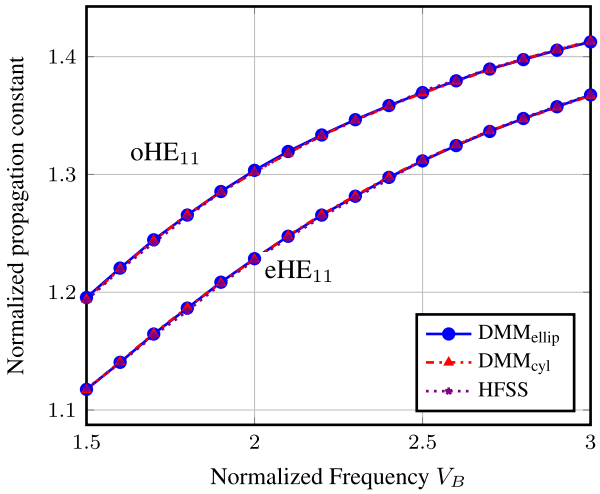

FIGURE 7. Dispersion curve of elliptical waveguide with anisotropic material.

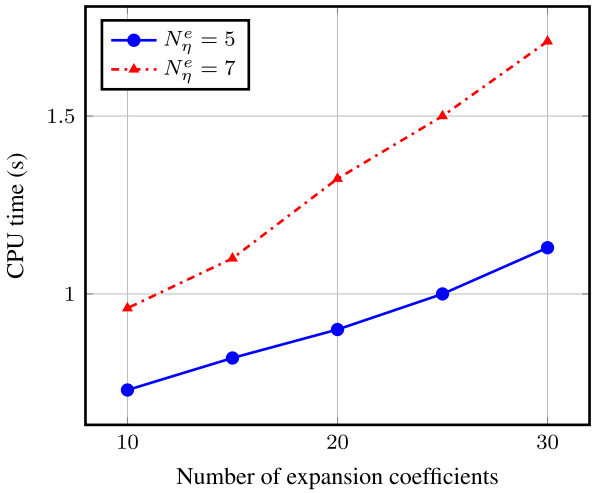

FIGURE 9. Time elapsed with varying expansion coefficients.

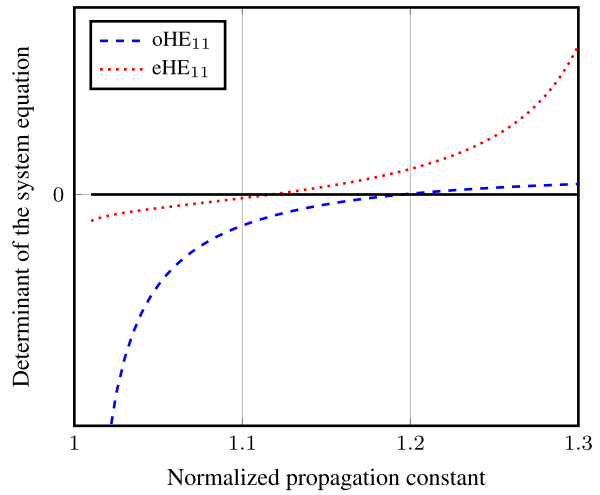

FIGURE 8. Numerical solution of the determinantal equation.

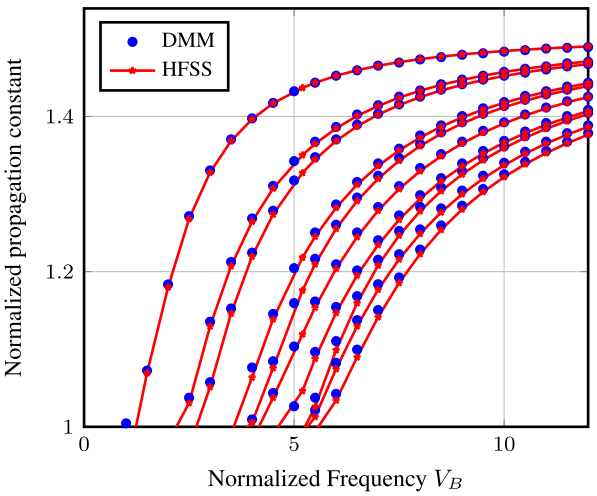

FIGURE 10. Higher order even modes of a dielectric rod.

The computed results agree very well with the open literature [4], [5], [17] and predicted results from ANSYS HFSS. We have used port mode calculation in HFSS and the computation time varied between 10 s to 38 s for V_B between 1.5 to 3. The results from [17] (MoL_{cyl}) are based on a cylindrical coordinate system while the results from [4] (MoL+Fourier) are calculated in an elliptical coordinate system but with Fourier approximation. We have also compared the results with those using a cylindrical coordinate system [13].

The programming of the codes has been done in MATLAB with Intel i7-6600U CPU @2.6 GHz processor. Fig. 9 shows the time required to compute even mode normalized propagation constant for isotropic case at $V_B = 1.5$. Only quarter of the structure has been analyzed for this computation. The computed propagation constants for all number of expansion coefficients are the same up to 8 decimals. For the cylindrical coordinate system, the computation time increases with the number of lines used for discretization. The time was from 0.6 s to 4.5 s for 7 to 25 e-lines on quarter of the structure.

B. INVESTIGATION OF HIGHER ORDER MODES

Further to investigate higher order modes, we have analyzed a polythene rod as elliptical core with $\varepsilon_r = 2.26$ and surrounded by air. We have done the computation with an axial ratio $B/A = 0.9$. Fig. 10 and 11 show the results for the even and odd fundamental modes, respectively, and the first nine higher order modes. We have again plotted the dispersion curves against the normalized frequency V_B. They show very good agreement with the results computed from ANSYS HFSS. They are also in order with the results shown in [5].

C. MULTILAYERED ELLIPTICAL WAVEGUIDE

We have then investigated a 4 layered elliptical waveguide consisting of 3 elliptical cylinders with same and different ellipticities as shown in Fig. 12. Outer layer of the structure is left open. The structure has been analyzed for both isotropic and anisotropic materials. The major axis of the inner layer of structure is with $A_0 = 4$ mm and minor axis is with $B_0 = 2$ mm. The width of the first layer in major axis direction is 0.5 mm and second layer is 0.6 mm.

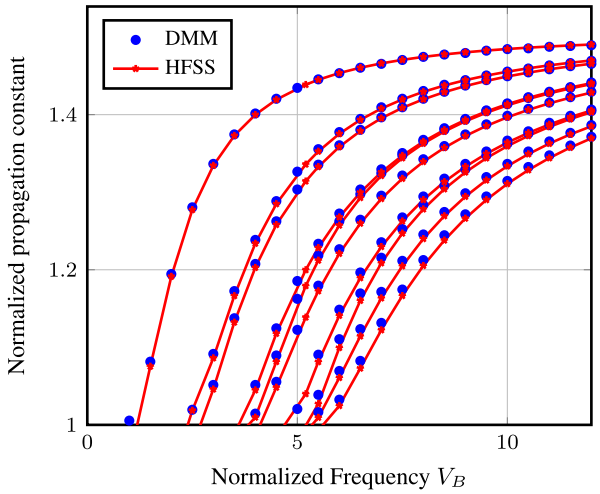

FIGURE 11. Higher order odd modes of a dielectric rod.

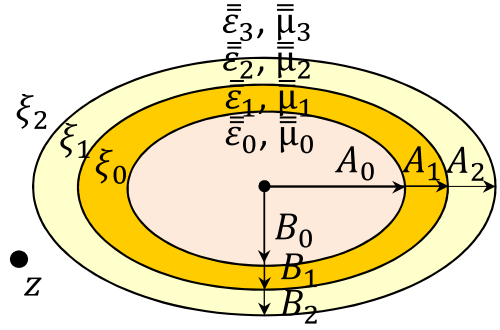

(a) Layers with equal ellipticities.

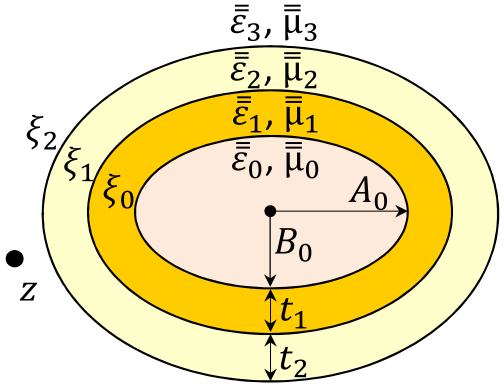

(b) Layers with different ellipticities.

FIGURE 12. Analyzed multilayered waveguide cross-section.

The structure consisting of dielectric layers with same ellipticities (Fig. 12a) has axial ratio of 0.5, therefore, $A_1 = 4.5$ mm, $B_1 = 0.5A_1$, $A_2 = 5.1$ mm and $B_2 = 0.5A_2$. For the structure with different ellipticities (Fig. 12b), we have taken thickness of the layers 1 and 2, i.e., t_1 and t_2, constant throughout η coordinate, therefore, $A_1 = 4.5$ mm, $B_1 = 2.5$ mm, $A_2 = 5.1$ mm and $B_2 = 3.1$ mm. The ξ-coordinate of the different layers can be calculated using $A = f\cosh\xi$ or $B = f\sinh\xi$. The material properties of the structure with isotropic dielectric layers are $\varepsilon_{r0} = 6$, $\varepsilon_{r1} = 3.5$, $\varepsilon_{r2} = 2$, $\varepsilon_{r3} = 1$ and $\mu_{r0} = \mu_{r1} = \mu_{r2} = \mu_{r3} = 1$. Whereas, the material properties of

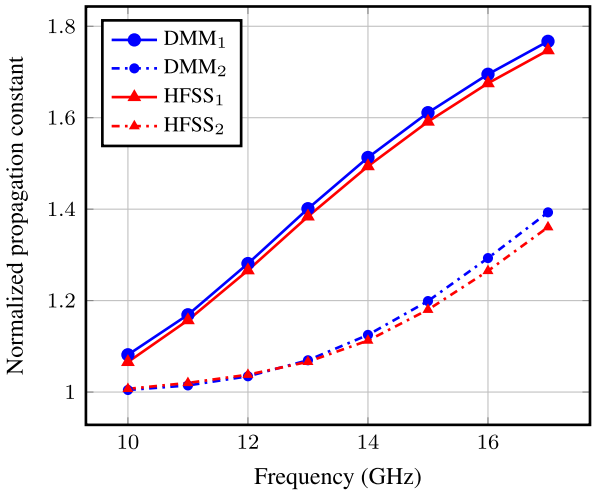

FIGURE 13. Dispersion curve of multilayered elliptical waveguide (same ellipticities) with isotropic material.

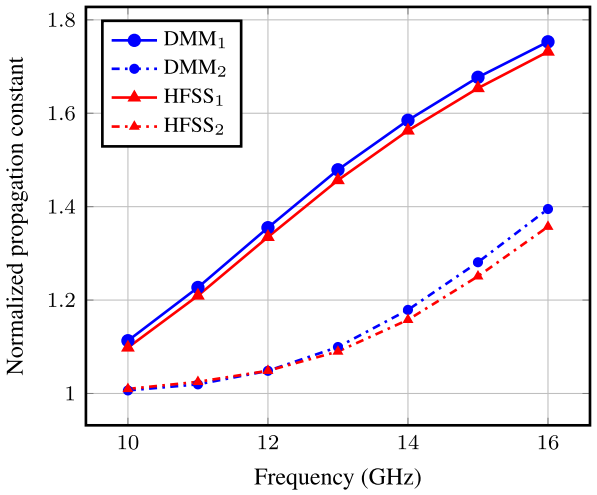

FIGURE 14. Dispersion curve of multilayered elliptical waveguide (same ellipticities) with anisotropic material.

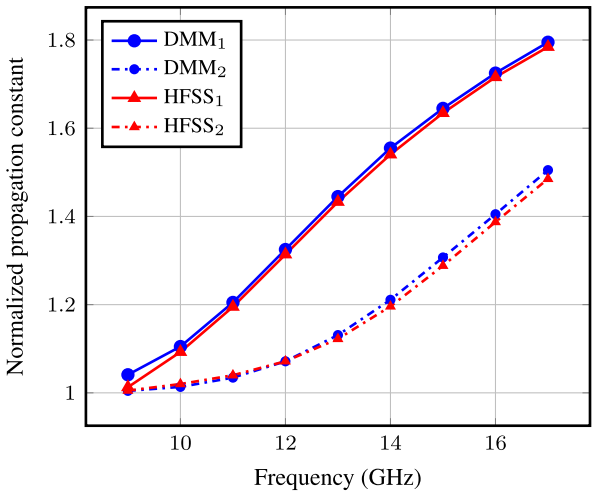

FIGURE 15. Dispersion curve of multilayered elliptical waveguide (different ellipticities) with isotropic material.

the structure with anisotropic dielectric layers are $\bar{\bar{\varepsilon}}_{r0} = (6, 6, 7)$, $\bar{\bar{\varepsilon}}_{r1} = (3.5, 3.5, 4)$, $\bar{\bar{\varepsilon}}_{r2} = (2, 2, 3)$, $\varepsilon_{r3} = 1$ and

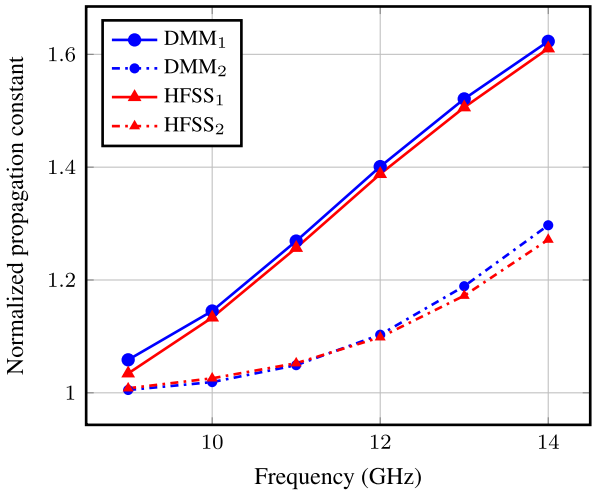

FIGURE 16. Dispersion curve of multilayered elliptical waveguide (different ellipticities) with anisotropic material.

$\mu_{r0} = \mu_{r1} = \mu_{r2} = \mu_{r3} = 1$. The dispersion curves of the both structures with isotropic and anisotropic materials are shown in Figs. 13-16. Both DMM and HFSS results are calculated for 2 top modes.

IV. CONCLUSION

Motivated with the conformal structures, we have discussed the DMM method with the elliptical coordinate system. The derivation of the hybrid matrix elements for anisotropic elliptical dielectric layers has been done. The formulation has been validated well with the quasi-cylindrical approach. The elliptical fibers have been analyzed with good agreement with the commercial software and open literature.

REFERENCES

[1] A. Antikainen, R.-J. Essiambre, and G. P. Agrawal, "Determination of modes of elliptical waveguides with ellipse transformation perturbation theory," *Optica*, vol. 4, no. 12, p. 1510, Dec. 2017.
[2] D. L. Young, S. P. Hu, C. W. Chen, C. M. Fan, and K. Murugesan, "Analysis of elliptical waveguides by the method of fundamental solutions," *Microw. Opt. Technol. Lett.*, vol. 44, no. 6, pp. 552–558, Mar. 2005. [Online]. Available: https://onlinelibrary.wiley.com/doi/abs/10.1002/mop.20695
[3] S. R. Rengarajan, "On higher order mode cutoff frequencies in elliptical step index fibers," *IEEE Trans. Microw. Theory Techn.*, vol. MTT-37, no. 8, pp. 1244–1248, Aug. 1989.
[4] O. Conradi and R. Pregla, "Analysis of fibers with elliptical cross section," in *Proc. 3rd Int. Conf. Transparent Opt. Netw.*, Nov. 2002, pp. 12–15.
[5] R. B. Dyott, *Elliptical Fiber Waveguides*. London, U.K.: Artech House, 1995.
[6] C. Yeh and F. I. Shimabukuro, *The Essence Dielectric Waveguides*. Boston, MA: Springer, 2008.
[7] A. Abdoli-Arani, "Optical properties of the electromagnetic waves propagating in an elliptical cylinder multilayer structure," *Chin. Phys. B*, vol. 23, no. 3, Mar. 2014, Art. no. 034211.
[8] A. Kusiek, R. Lech, W. Marynowski, and J. Mazur, "An analysis of multistrip line configuration on elliptical cylinder," *IEEE Trans. Microw. Theory Techn.*, vol. 63, no. 6, pp. 1800–1808, Jun. 2015.
[9] J. K. Shaw, W. M. Henry, and W. R. Winfrey, "Weakly guiding analysis of elliptical core step index waveguides based on the characteristic numbers of Mathieu's equation," *J. Lightw. Technol.*, vol. 13, no. 12, pp. 2359–2371, 1995.
[10] A. Dreher and A. Ioffe, "Analysis of microstrip lines in multilayer structures of arbitrarily varying thickness," *IEEE Microw. Guid. Wave Lett.*, vol. 10, no. 2, pp. 52–54, Feb. 2000.
[11] M. V. T. Heckler and A. Dreher, "Analysis of Conformal Microstrip Antennas With the Discrete Mode Matching Method," *IEEE Trans. Antennas Propag.*, vol. 59, no. 3, pp. 784–792, Mar. 2011.
[12] V. Kamra and A. Dreher, "Efficient analysis of multiple microstrip transmission lines with anisotropic substrates," *IEEE Microw. Wireless Compon. Lett.*, vol. 28, no. 8, pp. 636–638, Aug. 2018.
[13] V. Kamra and A. Dreher, "Analysis of circular and noncircular waveguides and striplines with multilayered uniaxial anisotropic medium," *IEEE Trans. Microw. Theory Techn.*, vol. 67, no. 2, pp. 584–591, Feb. 2019.
[14] N. W. McLachlan, *Theory Application Mathieu Functions*. Oxford, U.K.: Clarendon, 1951.
[15] J. E. Lewis and G. Deshpande, "Modes on elliptical cross-section dielectric-tube waveguides," *IEE J. Microw. Opt. Acoust.*, vol. 3, no. 4, pp. 147–155, Jul. 1979.
[16] V. Kamra and A. Dreher, "Full-wave equivalent circuit for the analysis of multilayered microwave structures with anisotropic layers," *Electron. Lett.*, vol. 54, no. 3, pp. 153–155, Feb. 2018.
[17] R. Pregla and O. Conradi, "Modeling of uniaxial anisotropic fibers with noncircular cross section by the method of lines," *J. Lightw. Technol.*, vol. 21, no. 5, pp. 1294–1299, May 2003.

VEENU KAMRA (Member, IEEE) was born in Bikaner, India, in 1990. She received the B.Tech. degree in electronics and communication engineering from Rajasthan Technical University, India, in 2012, and the M.Tech. degree in electronics and communication engineering (specialization in RF and microwaves) from the IITR, India, in 2014. She is currently pursuing the Ph.D. degree with the German Aerospace Center (DLR), Antenna Group, Institute of Communications and Navigation.

From August 2014 to January 2016, she worked as an Assistant Professor with the Jaipur Engineering College and Research Centre, India. Her current research interest includes numerical techniques for microwave structures.

ACHIM DREHER (Senior Member, IEEE) received the M.S. degree from Technische Universität Braunschweig, Braunschweig, Germany, in 1983, and the Ph.D. degree from the FernUniversität, Hagen, Germany, in 1992, both in electrical engineering.

From 1983 to 1985, he was a Development Engineer with Rohde and Schwarz GmbH and Co., KG, München, Germany. From 1985 to 1992, he was a Research Assistant, and from 1992 to 1997, he was a Senior Research Engineer with the Department of Electrical Engineering, FernUniversität. Since 1997, he has been with the German Aerospace Center (DLR), Institute of Communications and Navigation, Wessling, Germany, where he is currently the Head of the Antenna Research Group. His current research interests include analytical and numerical techniques for conformal antennas and microwave structures, smart antennas for satellite communications and navigation, and antenna technology for radar applications.

Dr. Dreher is a member of the VDE/ITG Expert Committee on Antennas, and he serves as a scientific coordinator and permanent lecturer of the Carl Cranz Series for Scientific Education in the areas of smart antenna systems.